DESIGN OF HIGH GAIN ULTRA WIDE-BAND ANTENNA FOR WIRELESS COMMUNICATION USING EBG STRUCTURES

A. Kaabal
S. Ahyoud
A. Asselman
Optics and Photonics Team, University Abdelmalek Essaadi,
Faculty of Science, Tetouan-Morocco
A. Faize
Communications System, University Abdelmalek Essaadi,
Faculty of Science, Tetouan-Morocco

Abstract

The properties of materials electromagnetic band-gap (EBG) and their advantage are being studied; then a high gain ultra-wideband (UWB) microstrip antenna using electromagnetic band-gap (EBG) structures concepts has been specifically designed in this paper. The -10 dB impedance bandwidth of the proposed antenna is 2.9–11.7 GHz about 251% broader, which is one of the most usable bandwidth regions for wireless applications such as WiMAX, WiFi outdoor, WLAN, Hiperlan and so on. The proposed antenna has an average gain of 6.6 dB and the peak is 18.99 dB at 4.19 GHz. The designing and simulation results done by using ANSOFT High Frequency Structure Simulator (HFSS), show that the antenna has higher gain than conventional UWB microstrip antenna.

Keywords: Electromagnetic Band Gap, antenna EBG, structure periodic, HFSS, ultra wide band

Introduction:

Often, we need devices that can concentrate the radiated energy in a particular direction. That's, a high gain and directivity. And for a strong application in the field of wireless communication such as WLAN (Wireless Local Area Network) band and WMAN (Wireless Metropolitan Area Network) and HiperLAN band. These devices must be less bulky. Using simple EBG substrate provides answers to the problem of congestion for this type of antenna, because this type of antenna has usually a relatively reduced thickness ($e < \lambda$) unlike many other focalized systems (parabolic antennas, cornets, lenses).

Rayleigh in 1887 shows that a periodic structure type Bragg mirror can create a frequency band within which any electromagnetic propagation is impossible (Yannick MERLE, 2003, Julien DROUET, 2007, Eric ARNAUD, 2010). EBG resonator antennas typically consist of an EBG material placed a half-wavelength above a ground plane containing a single source. The EBG material and ground plane form a single resonator that acts as a spatial filter to the source and creates highly gain and directional radiation characteristics. Several different types of EBG materials have been used to create these antennas, and the materials may be classified according to the dimensionality of the periodicity (Yannick MERLE, 2007). In 1987, E. Yablonovitch and S. John extend the concept of Bragg mirrors in 2 and 3 dimensions (E. Yablonovitch, 1993, E. Yablonovitch, 2000, S. John, 1987, A. M. M.PLIHAL,1991, M. P.R VILLENEUVE,1992, JIN Chong-jin et al. , 1999, Alexander J. Glass, 2005). The propagation of electromagnetic waves within these materials generates strong interactions with the components of materials. As soon as the wavelength becomes less than spatial period of material, the laws of propagation become dispersive and anisotropic. This creates spatial and frequency filtering, creating the bandgap (Julien DROUET, 2007).

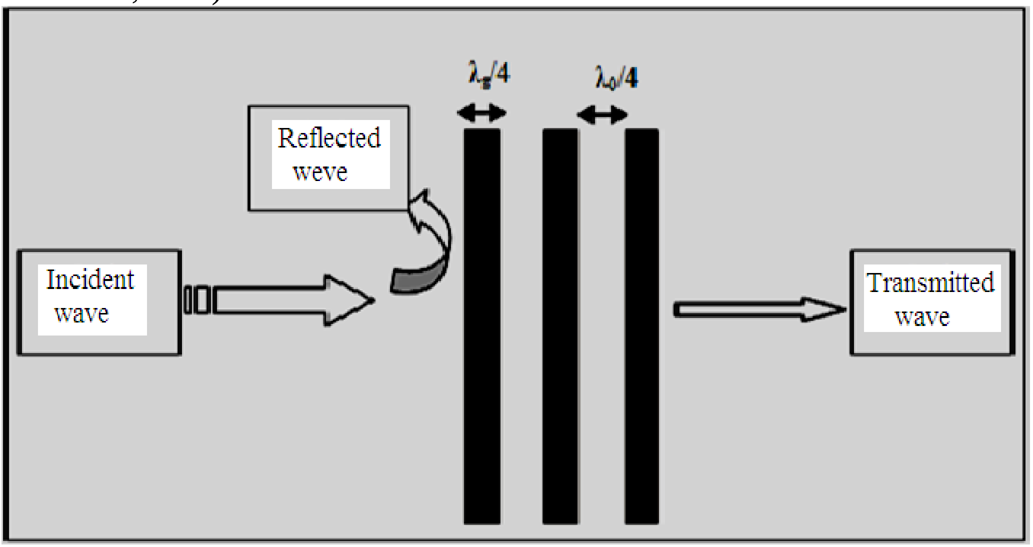

Figure 1: representation schematic of a Bragg mirror consists of two types of layers; one of permittivity εr and the other is air.

Theory

The Maxwell’s equations for an electromagnetic wave propagating through a dielectric medium with no free charge or current are given by:

$\overrightarrow{rot}\ \vec{E} = -\mu \frac{\partial \vec{H}}{\partial t}$ (1)

$\overrightarrow{rot}\ \vec{H} = \epsilon \frac{\partial \vec{E}}{\partial t}$ (2)

$\text{div}\ \vec{E} = 0$ (3)

$\text{div}\ \vec{H} = 0$ (4)

Where the time dependence of the electromagnetic field has been taken to be:

$\vec{E}(\vec{r},t) = \vec{E}(\vec{r})e^{-i\omega t}$ (5)

$\vec{B}(\vec{r},t) = \vec{B}(\vec{r})e^{-i\omega t}$ (6)

Combining now the Maxwell's equations, we get the second-order differential equation for the electric field which satisfies the equation in each layer:

$\Box\vec{E} + \frac{\omega^2 . \epsilon_r(x,y,z)}{c^2}\vec{E} = \vec{0}$ (7)

Where *c* is the vacuum speed of light and $\epsilon_r(x, y, z)$ is the permittivity for the layer.

In a one-dimensional system of a periodicity along the *z*-axis, the equation (7) becomes:

$\frac{\partial^2 E(z)}{\partial z^2} + \frac{\omega^2 . \epsilon_r(z)}{c^2} E(z) = 0$ (8)

And as the permittivity ϵ_r(z) is periodic with period *d*, it is possible to highlight the notion of allowed bands and bandgaps again. Thus, the equation (8) can be solved by considering a one-dimensional periodic lattice. The shape of the permittivity ϵ_r(z) is described in the figure (2).

If $0 < x < a$ then $\epsilon_r(z) = 1$ and $\frac{\partial^2 E_{AB}(z)}{\partial z^2} + \frac{\omega^2}{c^2} E_{AB}(z) = 0$ (9)

If $a < x < a + d$ then $\epsilon_r(z) = \epsilon_r$ and $\frac{\partial^2 E_{BC}(z)}{\partial z^2} + \frac{\omega^2 . \epsilon_r}{c^2} E_{BC}(z) = 0$ (10)

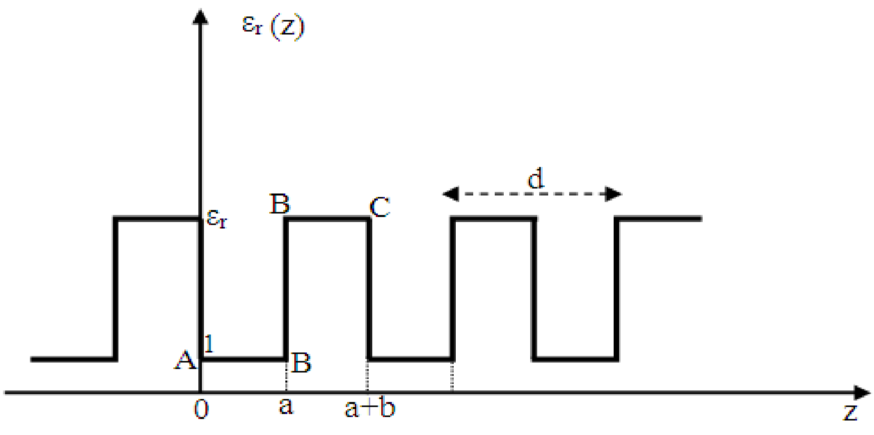

Figure 2: periodic dielectric constant $\epsilon_r(z + d) = \epsilon_r(z)$

The previous solutions of differential equations are respectively:

$$E_{AB}(z) = A\cos(\alpha z) + B\cos(\alpha z) \quad (11)$$

$$E_{BC}(z) = C\cos(\beta z) + D\cos(\beta z) \quad (12)$$

With $\beta = \frac{\omega}{c}\sqrt{\epsilon_r}$ and $\alpha = \frac{\omega}{c}$

Using the fact that at point B the function E (z) and its derivative E (z) are continuous, and the $\epsilon_r(z)$ is periodic, and that the electric field E (z) which satisfies the equation (8) has a Bloch function solution of $E(z) = u(z)e^{jkz}$ (13)

Where u(z) is a periodic function with the same period *d* as the permittivity distribution; that's, u (z + d) = u (z), and *k* is a constant wavelength. Thus, it is possible to easily show the following dispersion relation:

$$\cos(\alpha a)\cos(\beta b) - \sin(\alpha a)\sin(\beta b)\frac{\epsilon_r + 1}{2\sqrt{\epsilon_r}} = \cos[k(a + b)] \quad (14)$$

The figure 3 shows that the left side of the equality can be greater than 1 or less than -1, but the second member is always between -1 and +1. In this case, there is no wave vector k which satisfies the dispersion relation. So, no electromagnetic wave propagates. Such as α and β both depend on the pulse ω, then we talk about a forbidden band of frequencies. So the one-dimensional periodic material prevents electromagnetic waves from spread in these considered frequencies.

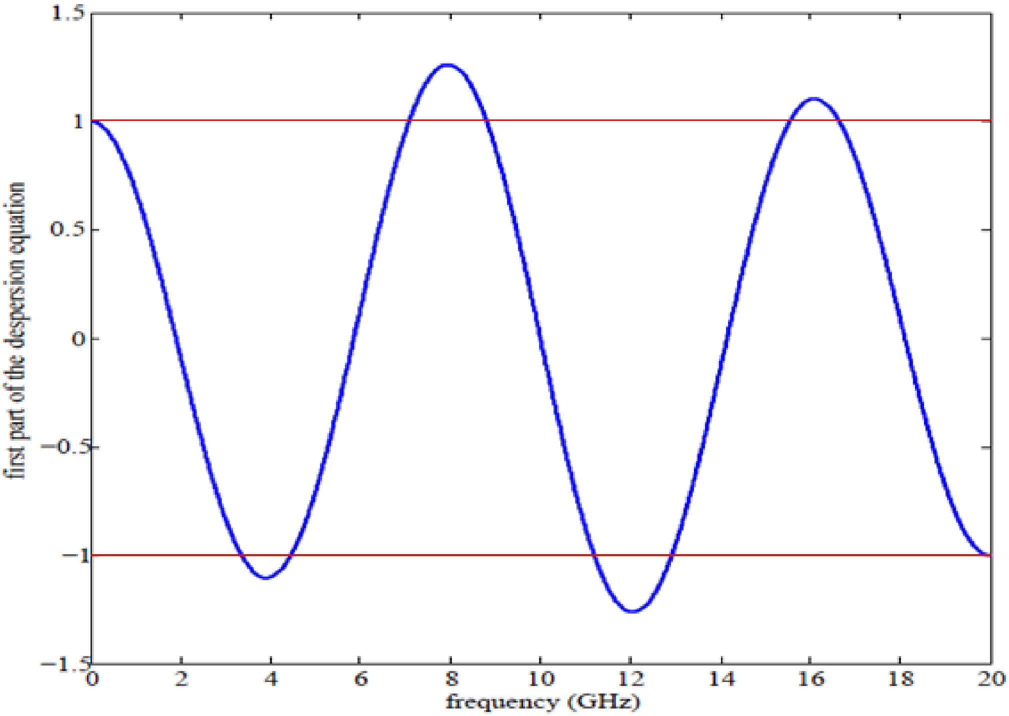

Figure 3: dispersion diagram

In order to solve the photonic band equation, and for antenna application, we need to compute the reflection coefficient Γ and the transmission coefficient T. This is most simply computed by using the transfer-matrix method as outlined below, a method that is quite familiar in the treatment of light transmission in layered media. We first divide the cell into a large number N of segments along z such that the refractive index in each layer may be considered to be a constant. For each of the two modes TE or TM, the electromagnetic fields at the left and right end of the layer are related via the 2×2 transfer matrix M_i .

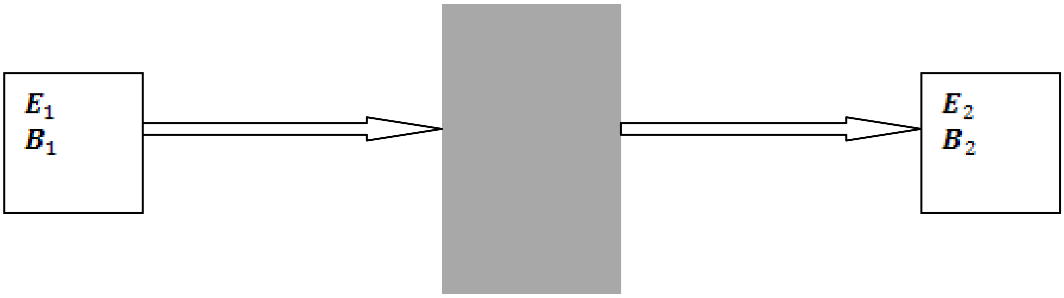

Figure 4: Sketch of the each layer

$$\begin{bmatrix} E_1 \\ B_1 \end{bmatrix} = M_i \begin{bmatrix} E_2 \\ B_2 \end{bmatrix} \qquad (15)$$

Since E_i and B_i are the tangential components of the electromagnetic field on the left and right sides of the unit cell.

Where: $$M_i = \begin{bmatrix} \cos\delta_i & i\sin\delta_i/\gamma_i \\ i\gamma_i\sin\delta_i & \cos\delta_i \end{bmatrix} \qquad (16)$$

With: $$\delta_i = -d_i k_i \qquad (17)$$

$$\gamma_i = \begin{cases} \frac{k_i}{\omega} & (TE) \\ \frac{\left(\frac{n_i}{c}\right)^2}{\frac{k_i}{\omega}} & (TM) \end{cases} \qquad (18)$$

$k_i = \left(\frac{\omega}{c}\right) n_i$ in the case of normal incidence, n_i is the refractive index of the ith layers , d_i is its thickness, and c is the vacuum speed of light.

The overall transfer matrix corresponding to the entire unit cell, treated as a multilayer stack consisting of *N* segments, is the product of the individual transfer matrices:

$$M = \begin{bmatrix} m_{11} & m_{12} \\ m_{21} & m_{22} \end{bmatrix} = \lim_{N\to\infty} \prod_{i=1}^{N} M_i \qquad (19)$$

The transmission and the reflection coefficients for the entire multilayer stack may be written in terms of the following two quantities:

$$T = \frac{2\Gamma_0}{\Gamma_0 m_{11} + \Gamma_0{}^2 m_{12} + m_{21} + \Gamma_0 m_{22}} \qquad (20)$$

$$\Gamma = \frac{\Gamma_0 m_{11} + \Gamma_0{}^2 m_{12} - m_{21} - \Gamma_0 m_{22}}{\Gamma_0 m_{11} + \Gamma_0{}^2 m_{12} + m_{21} + \Gamma_0 m_{22}} \quad (21)$$

$\Gamma_0 = \frac{n_0}{c}$ corresponds to the tail region, n_0 being the refractive index at the two edges of the unit cell.

Results and discussion

Using a Bragg mirror constitutes of dielectric plates FR4_epoxy with a permittivity ε_r=4.4 and thickness correspond the frequency f_0=10GHz, the plates are separated with layers of air. This structure will interact with an external electromagnetic aggression, we have an interaction with a normal incident plane wave propagating at the resonant frequency f_0. The diffracted waves are characterized by the transmission or reflection coefficients (figure 5).

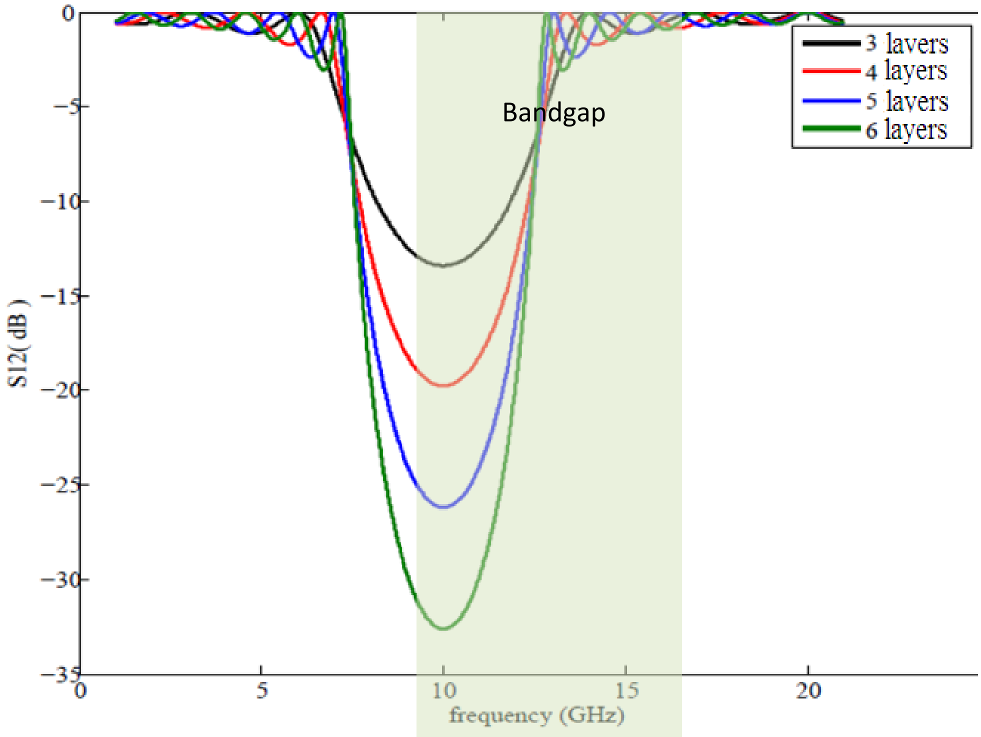

Figure 5: Influence on plate number of the transmission coefficient of a structure without default.

It is observed the presence of a frequency band prohibiting transmission of electromagnetic waves centered at f_0, called bandgap. The depth and width of the band gap depends on the number plates of the EBG structure, when the number of plates increases, the well of transmission becomes deeper and narrower, this is due to multiple reflections on the dielectric plates.

To apply the EBG in antennas, the properties of resonant structures EBG it used (Eric ARNAUD, 2010, Yannick MERLE, 2003). This analysis leads to the development guideline EBG materials antenna. The first step of the design is the construction of a cavity in the middle of a multilayer structure EBG corresponds to the wavelength at which the transmission in the EBG is prohibited. Figure 6 shows the transmission and reflection coefficient for a structure has six layers. In this way, we obtain a resonant structure that resembles the Fabry-Perot cavity.

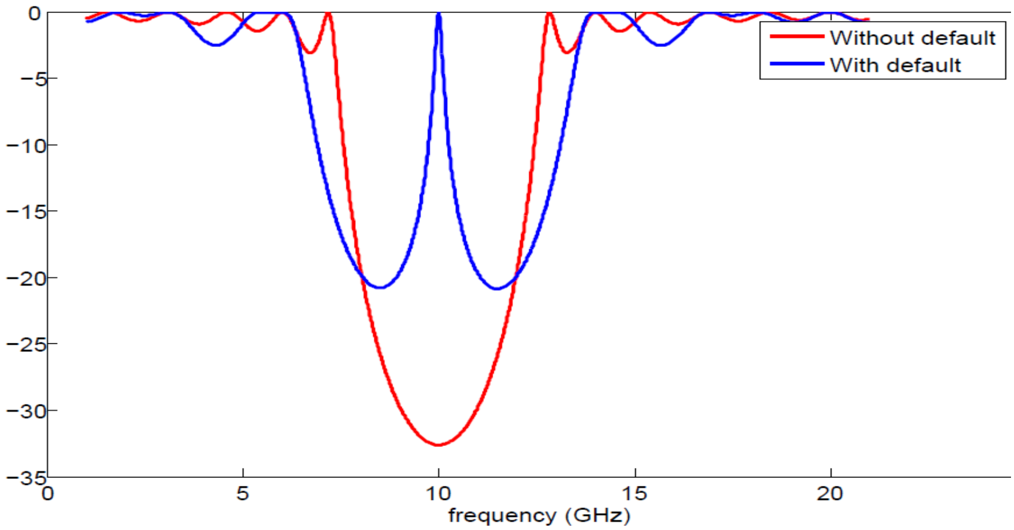

(a)

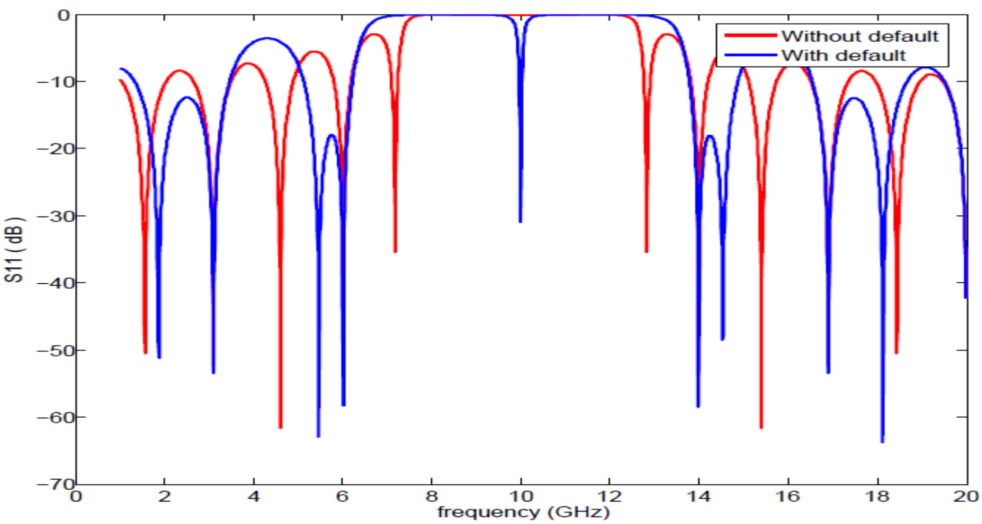

(b)

Figure 6: Influence of structure EBG 1D with and without default on
(a) Transmission coefficient
(b) reflection coefficient.

Zeros (dB) of the transmission coefficient translate resonance phenomena, can be also extracted of peaks draw zero bending (< -30 dB) of reflection coefficient. A transmission peak is formed at the center frequency f_0 of the bandgap, so to use the EBG antenna structure it is interesting to introduce default in the structure. This phenomenon of frequency filtering is exploited for EBG antenna design by introducing an excitation in the default. These materials also allow spatial filtering since it is possible to favor one direction of radiation in space when combined with an antenna. For radiation in one direction introducing a ground plane in the middle of the defect, and EBG material positioned above the ground plane with λ_0 / 2.

This paragraph shows that the periodicity of the dielectric permittivity can prevent the propagation of waves in a certain frequency band. This notion of frequency can be extended to 2 or 3 dimensions, but the nature of the vector equation spread considerably complicates the theoretical resolution of the problem.

Antenna design and results

In figure 4 the top and bottom views of the UWB antenna is shown as well as its dimensions. The antenna was constructed on an h = 0.8mm Rogers RO4003 (tm) substrate with a relative permittivity ϵ_r = 3.55 and a loss tangent tanδ = 0.002.

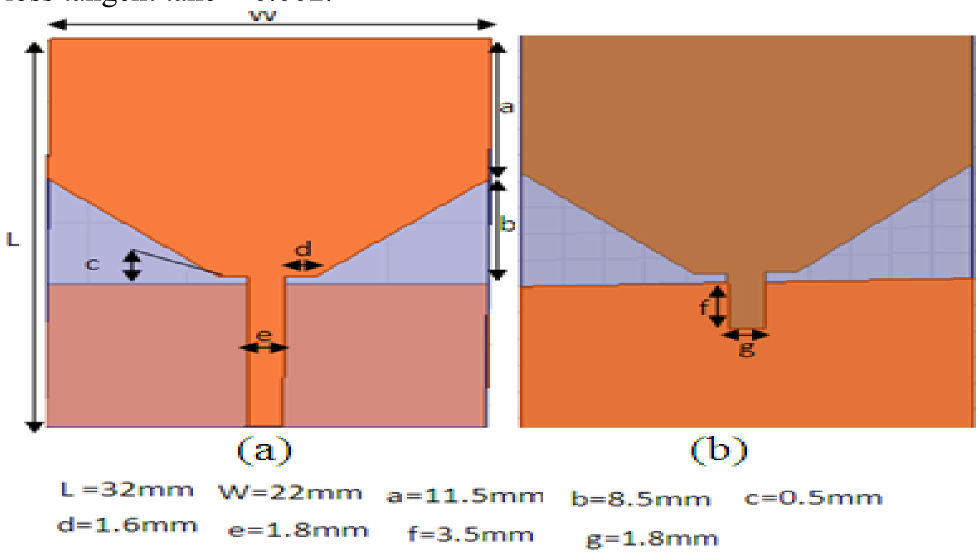

Figure 7: The characteristic of antenna (a) top view (b) bottom view.

The result is obtained by using HFSS. A patch antenna radiator is fed by a 50Ω microstrip line. The microstrip feed line source itself is fed by *Lumped Port*. The model area is surrounded by an absorbent box ABC (absorbing boundary condition). The figure 8 shows that antenna obtains a good impedance matching in an ultra width-band.

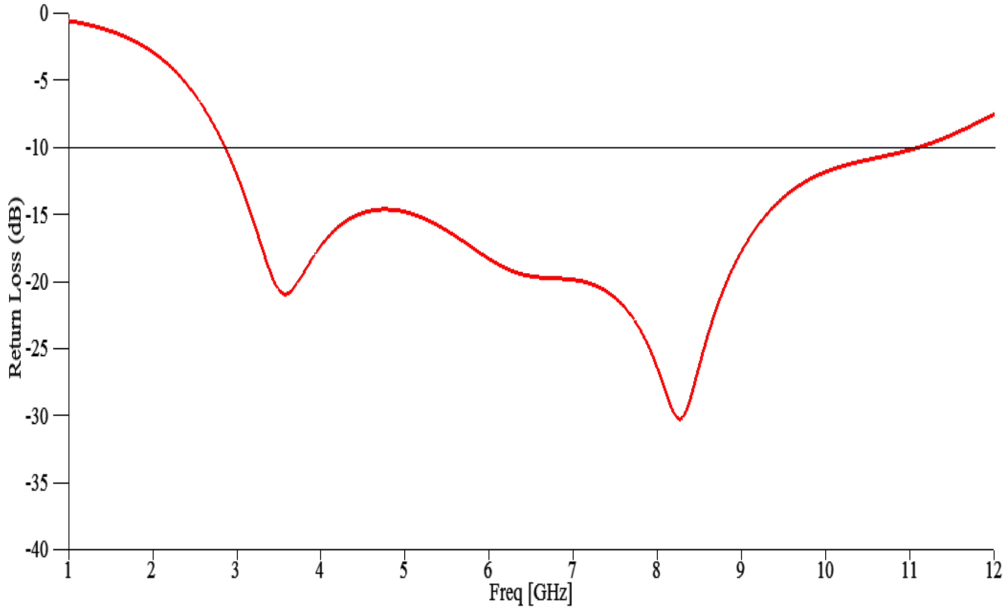

Figure 8: Variation of return loss

A resonant cavity composed of EBG material is added above UWB antenna to increases the gain. Figure 9 shows the proposed UWB antenna using EBG structures consists of three layers of FR4_epoxy substrate with a relative permittivity $\epsilon_r = 4.4$.

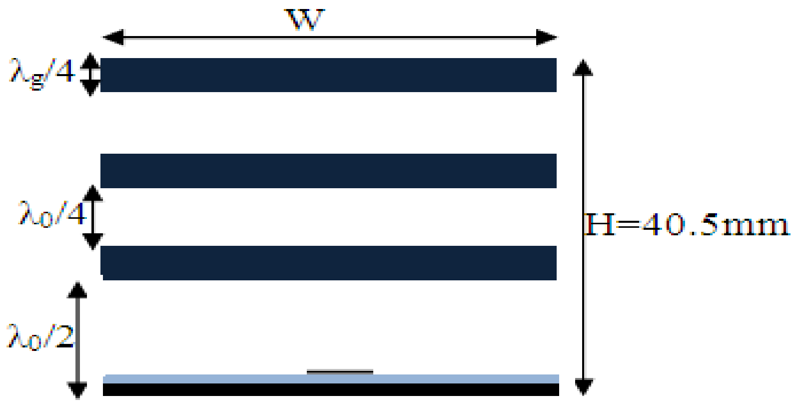

Figure 9: antenna Ultra With Band using EBG structures

The figure 10 shows the impedance bandwidth of the proposed antenna, and that's operating at the entire UWB band (3.1GHZ to 10.6 GHz) for a wireless communication.

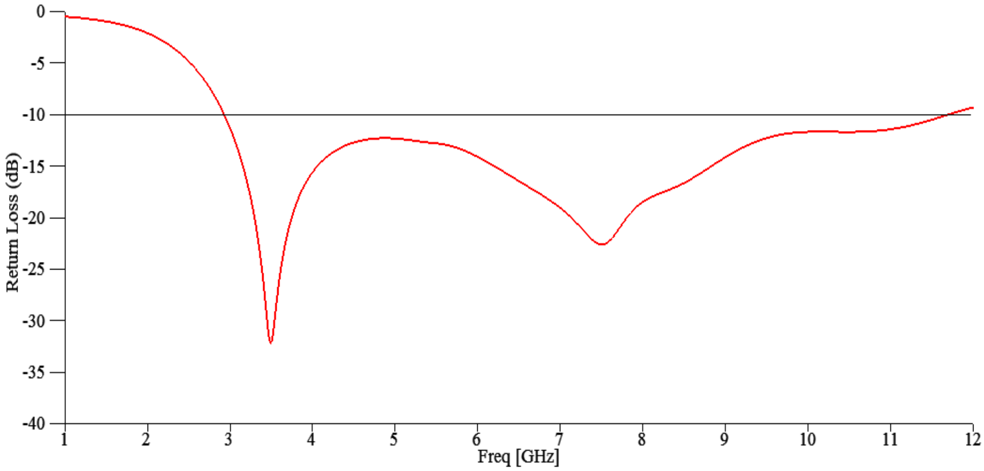

Figure 10: Return loss of the UWB antenna using EBG.

Moreover, the gain of EBG antenna has increased by a considerable amount of 16.58 dBi at 4.19 GHz compared with the simple ultra wide band antenna at the same frequency. The gain for the two antennas were calculated between the impedance bandwidth (2.93 – 11.72 GHz) as shown in Figure 11.

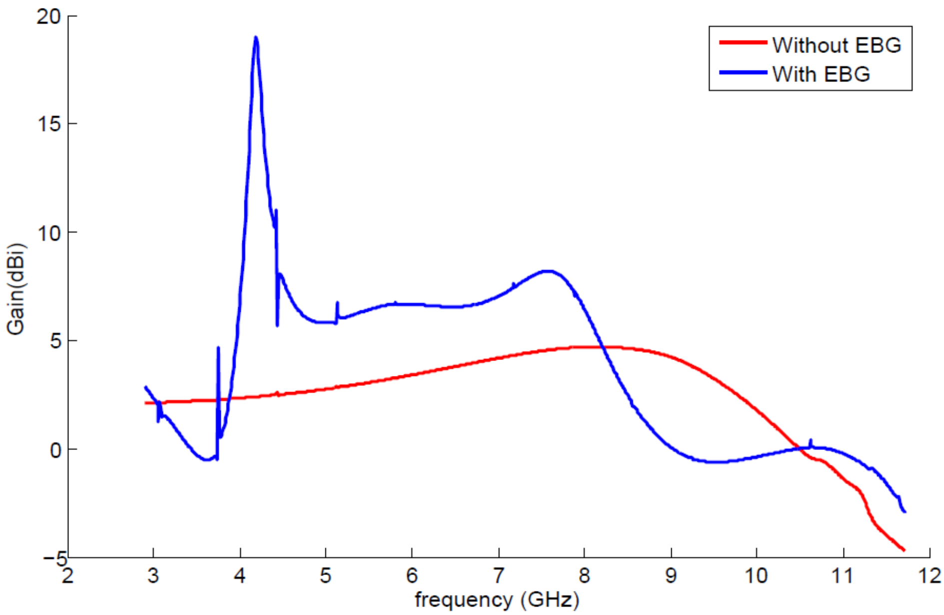

Figure 11: simulated gain for the designed antenna

From Figure 11 we found increased gain significantly between 3.88 and 8.21 GHz compared with the antennas using a mushroom-like EBG in (Pradeep Kumar et al.,2013, Lin Peng and Chengli Ruan,2013) where the gain does not exceed 5.7 dBi in this band. This increase in gain is actually due to reflections in the EBG structure, because the EBG structure is the spatial filter that can focus on one or more principal directions of radiation while filtering the other.

Conclusion:

A compact UWB antenna based on EBG structure composed of triple layers EBG cavity has been realized and discussed with detailed analysis in this paper. A significant improvement in gain between 3.88 and 8.21 GHz is shown in this paper. The antenna proposed can be expected to be a good candidate for use in the wireless communication.

References:

E. Yablonovitch (1993) , ‘‘ Photonic band-gap structures ’’, J. Opt. Soc. Am. B, Vol. 10,No. 2, pp. 283-295.

E. Yablonovitch (2000), ‘‘How to Be Truly Photonic ’’, Applied Physics. Vol. 289. no. 5479, pp. 557 – 559.

S. John (1987), “Strong localization of photons in certain disordered dielectric superlattices”, Physical Review, vol. 58.

A. M. M.PLIHAL (1991), “Photonic band structure of two dimensional systems: the triangular lattice”, Physical Review, vol. 44.

M. P.R VILLENEUVE (1992), “Photonic band gap in two dimensional square lattice: Square and circular rods”, Physical Review, vol. 46.

JIN Chong-jin et al. (1999), ‘‘A novel Two-Dimensional Photonic Crystal’’, Chin. Phys. Lett. Vol 16 No. 1, pp. 20-22.

Alexander J. Glass (2005), ‘‘Non-Optical Applications of Photonic Crystal Structures’’, A Report to the US Air Force Office of Scientific Research, University of New Mixico.

Julien DROUET (2007), ‘‘Méthodes d’analyse électromagnétique spécifiques à la conception des antennes à résonateur BIE multi sources’’, Thèse, Université de Limoges, France.

Eric ARNAUD (2010), ‘‘Contribution à la conception d’antennes B.I.E métalliques à polarisation circulaire alimentées par cornet’’, Thèse, Université de Limoges, France.

Yannick MERLE (2003), ‘‘Etude de la dispersion électromagnétique dans les matériaux périodiques diélectriques bidimensionnels’’, Thèse, Université de Limoges, France.

Pradeep Kumar et al.(2013), “Realization of Band-Notch UWB Monopole Antenna Using AMC Structure”, International Journal of Engineering and Technology. Vol.5, No.3.

Lin Peng and Chengli Ruan (2013), “Design and time-domain analysis of compact multi-band-notched UWB antennas with EBG structures”, Progress In Electromagnetics Research B, Vol. 47, pp. 339-357.